



HAL
open science

Heterozygous Mutations in BMP6 Pro-peptide Lead to Inappropriate Heparin Synthesis and Moderate Iron Overload in Humans

Raed Daher, Caroline Kannengiesser, Dounia Houamel, Thibaud Lefebvre, Edouard Bardou-Jacquet, Nicolas Ducrot, Caroline De Kerguenec, Anne-Marie Jouanolle, Anne-Marie Robreau, Claire Oudin, et al.

► To cite this version:

Raed Daher, Caroline Kannengiesser, Dounia Houamel, Thibaud Lefebvre, Edouard Bardou-Jacquet, et al.. Heterozygous Mutations in BMP6 Pro-peptide Lead to Inappropriate Heparin Synthesis and Moderate Iron Overload in Humans. *Gastroenterology*, 2016, 150 (3), pp.672-683. 10.1053/j.gastro.2015.10.049 . hal-01231430

HAL Id: hal-01231430

<https://univ-rennes.hal.science/hal-01231430>

Submitted on 22 Jan 2016

HAL is a multi-disciplinary open access archive for the deposit and dissemination of scientific research documents, whether they are published or not. The documents may come from teaching and research institutions in France or abroad, or from public or private research centers.

L'archive ouverte pluridisciplinaire **HAL**, est destinée au dépôt et à la diffusion de documents scientifiques de niveau recherche, publiés ou non, émanant des établissements d'enseignement et de recherche français ou étrangers, des laboratoires publics ou privés.

Heterozygous Mutations in BMP6 Pro-peptide Lead to Inappropriate Hcpidin Synthesis and Moderate Iron Overload in Humans

Running title: *BMP6*, gene for moderate hemochromatosis

Raed Daher^{1,2,3*}, Caroline Kannengiesser^{1,2,3,4*}, Dounia Houamel^{1,2,3*}, Thibaud Lefebvre^{1,2,3,5}, Edouard Bardou-Jacquet⁶, Nicolas Ducrot^{1,2,3}, Caroline de Kerguenec⁷, Anne-Marie Jouanolle^{6,8}, Anne-Marie Robreau⁵, Claire Oudin⁵, Gerald Le Gac⁹, Boualem Moulouel¹, Veronique Loustaud-Ratti¹⁰, Pierre Bedossa^{1,11}, Dominique Valla⁷, Laurent Gouya^{1,2,3,5}, Carole Beaumont^{1,2,3}, Pierre Brissot⁶, Hervé Puy^{1,2,3,5}, Zoubida Karim^{1,2,3**} and Dimitri Tchernitchko^{4**}

¹ INSERM UMR1149, Centre de Recherche sur l'inflammation, Paris, France. ² Université Paris Diderot, site Bichat, Sorbonne Paris cité, Paris, France. ³ Laboratory of excellence, GR-Ex, Paris, France. ⁴ AP-HP, Département de Génétique, Hôpital Bichat, Paris, France. ⁵ AP-HP, Centre Français des Porphyries, Hôpital Louis Mourier, Colombes, France. ⁶ CHU Rennes, Liver disease and Molecular Genetics departments, Rennes, France. ⁷ AP-HP, Département d'Hépatologie, Hôpital Beaujon, Clichy, France. ⁸ CHU Rennes, French reference centre for rare iron overload diseases of genetic origin. ⁹ Inserm U1078, Université de Brest, CHRU de Brest, Laboratoire de Génétique Moléculaire et d'Histocompatibilité, Bretagne, Brest, France. ¹⁰ Service d'Hépatogastroentérologie, INSERM UMR1092, Limoges, France. ¹¹ AP-HP, Laboratoire d'Anatomo-pathologie, Hôpital Beaujon, Clichy, France.

* These authors contributed equally to the work

** These two senior authors contributed equally to the work

Corresponding author: Zoubida Karim, PhD

INSERM U1149. Université Paris Diderot, site Bichat, 16 rue Henri Huchard, 75018 Paris, France.

E-mail: zoubida.karim@inserm.fr

AUTHOR CONTRIBUTIONS

Study concept and design: C.K, D.T., Z.K.; acquisition of the first cohort and patients data: C.D.K., D.V, C.K. H.P; patients' DNA sequencing: A.M.R., C.O., DT, C.K. Analysis and interpretation of patient data: H.P., C.B.; Study supervision: Z.K.; critical revision of the manuscript for important intellectual content: Z.K., H.P., C.B. statistical analysis: L.G., D.T.; conducting experiments or material support: Z.K., D.H., R.D., T.L., N.D., P.B., D.T., G.L., B.M.; Drafting of the manuscript: D.T., C.B., Z.K.; acquisition of the cohort replication and data: E.B.J, A.M.J, V.L.R., P.B. All authors participated in data discussion, read and approved the manuscript.

ACKNOWLEDGEMENTS

We are very grateful to all patient families who kindly contributed to this study. We thank Samira Benadda for confocal microscopy assistance. INSERM and Paris Diderot University, France supported this work. Dounia Houamel and Raed Daher were supported by the Laboratory of excellence, GR-Ex, Paris, France. The labex GR-Ex, reference ANR-11-LABX-0051 is funded by the program "Investissements d'avenir" of the French National Research Agency, reference ANR-11-IDEX-0005-02. Dounia Houamel was additionally supported by Paris Diderot University, the "Société Française d'Hématologie". Boualem Moulouel was supported by a grant from the « Fondation pour la Recherche Médicale Française ».

No potential conflict of interest relevant to this article was reported.

Abstract:

BACKGROUND & AIMS: Hereditary hemochromatosis is a heterogeneous group of genetic disorders characterized by parenchymal iron overload. It is caused by defective expression of liver hepcidin, the main regulator of iron homeostasis. Iron stimulates the gene encoding (HAMP) hepcidin via the BMP6 signaling to SMAD. Although several genetic factors have been found to cause late-onset hemochromatosis, many patients have unexplained signs of iron overload. We investigated BMP6 function in these individuals.

METHODS: We sequenced the BMP6 gene in 70 consecutive patients with moderate increase in serum ferritin and liver iron who did not carry genetic variants associated with hemochromatosis. We searched for BMP6 mutations in relatives of 5 probands and in 200 healthy individuals (controls), as well as in two other independent cohorts of hyperferritinemia patients.

We measured serum levels of hepcidin by liquid chromatography-tandem mass spectrometry and analyzed BMP6 in liver biopsies from patients by immunohistochemistry. The functions of mutant and normal BMP6 were assessed in transfected cells using immunofluorescence, real-time quantitative PCR, and immunoblot analyses.

RESULTS: We identified 3 heterozygous missense mutations in BMP6 (p.Pro95Ser, p.Leu96Pro, and p.Gln113Glu) in 6 unrelated patients with unexplained iron overload (9% of our cohort). These mutations were detected in less than 1% of controls. The p.Leu96Pro was also found in 2 patients from the additional cohorts. Family studies indicated dominant transmission. Serum levels of hepcidin were inappropriately low in patients. A low level of BMP6, compared with controls, was found in a biopsy from 1 patient. In cell lines, the mutated residues in the BMP6 propeptide resulted in defective secretion of BMP6; reduced signaling via SMAD1, SMAD5, and SMAD8; and loss of hepcidin production.

CONCLUSIONS: We identified 3 heterozygous missense mutations in BMP6 in patients with unexplained iron overload. These mutations lead to loss of signaling to SMAD proteins and reduced hepcidin production. These mutations might increase susceptibility to mild-to-moderate late onset iron overload.

KEYWORDS: genetic analysis, bone morphogenetic protein, signal transduction, HH

INTRODUCTION

Hereditary hemochromatosis (HH) is an iron overload disorder reflecting mutations in different genes encoding proteins involved in the regulation of hepcidin production. Hepcidin acts as a negative regulator of duodenal iron intake [1] and iron recycling from spleen and liver macrophages [2,3]. HH is characterized by abnormal iron loading in parenchyma, leading to liver cirrhosis, cardiomyopathy, diabetes, hypogonadism and arthralgia [4,5] although only a few HH patients suffer from overt disease. Currently, the main therapeutic approach is a regular phlebotomy to remove excess iron [6].

Hepcidin synthesis in the liver is controlled by serum iron levels and tissue iron stores through an “iron-sensing complex” comprising the integral proteins HFE, hemojuvelin (HJV) and the type 2-transferrin receptor (TFR2). This complex acts through the bone morphogenetic protein (BMP)/SMAD1/5/8-signaling complex to induce hepcidin-encoding gene (*HAMP*) expression when too much iron is available [7]. Hepcidin synthesis is also induced by inflammatory signals such as IL-6 and plays a major role in the anemia of chronic diseases [8,9]. In contrast, *HAMP* gene is negatively regulated through the serine protease matriptase 2, which cleaves HJV and disrupts BMP/SMAD signaling [10-12]. In European Caucasian populations, *HFE* is responsible for the most common form of adult-onset HH, while *HAMP*, *HJV* and *TFR2* genes are responsible for the rare (<1 %) early-onset subtypes of HH, showing the rapid and severe progression of iron overload [5,13]. In rare cases, dominant mutations in the iron exporter ferroportin (*FPN*) gene can also lead to an iron overload phenotype [14-17]. Nevertheless, there are many patients with iron overload in whom no causative mutation in the known hemochromatosis genes has been identified [18].

BMPs belong to the TGF- β family and are involved in both osteogenic (bone and cartilage) and non-osteogenic developmental processes [19]. The *BMP6* gene (6p24-p23) has seven exons, encoding a large precursor of 513 amino acids (aa), comprising an N-terminal signal peptide sequence, a prodomain for proper folding, and a C-terminal secreted mature peptide sequence of 138 aa (Figure 1A). BMP6 is also a key regulator of hepcidin expression and iron metabolism [20-22]. This protein cooperates with HJV to bind to BMP type I and type II receptors and induces the phosphorylation of SMAD 1/5/8 proteins, which subsequently interact with SMAD4. This complex translocates to the nucleus, where it binds the *HAMP* promoter and stimulates *HAMP* gene transcription. Recent studies have shown that *Bmp6*-deficient mice develop a severe iron overload [20,22], suggesting that *BMP6* might be a candidate gene in patients with severe HH not attributable to *HJV* or *HAMP* genes [20,22]. However, because no BMP6 mutations have been reported, we postulated that, in humans, these mutations might be responsible for a mild late-onset phenotype rather than severe iron overload phenotype. Therefore, we analyzed the *BMP6* gene in a series of 70 patients with primary mild to moderate iron overload in whom mutations in known HH

genes had been excluded. Identified BMP6 mutations were additionally found in two other independent cohorts of hyperferritinemia patients.

MATERIALS and METHODS

BMP6 gene 7 exons and flanking sequences were sequenced in 70 consecutive patients (51 males and 19 females) and 200 healthy controls (blood donors over 35 years old, 108 males and 92 females). The patients were referred to the Department of Genetics in Bichat Hospital (Paris, France) between 2004 and 2011 for the screening of primary non-HFE hemochromatosis (see supplementary Table S1) and presented with high ferritinemia and elevated liver iron concentration (LIC > 36 $\mu\text{mol/g}$ as confirmed through Magnetic Resonance Imaging (MRI) analysis). Cases with hyperferritinemia of known origin were excluded: chronic or acute inflammatory syndrome, transfusions, cellular lysis, dysmetabolic syndrome, and excessive alcohol consumption. Genetic analyses had previously ruled out defects in *HFE* (C282Y homozygous, compound C282Y/H63D heterozygous), *TFR2* and *FPN* genes. Serum hepcidin was measured in all samples with a previously validated LC-MSMS method [23].

All patients and healthy controls were Caucasians of western continental French descent, originating from the Ile de France region. Written informed consent was obtained for all participants, and this study was approved through the local ethical committees.

The replication cohort consisted of a prospective nationwide study from 2011 to 2013. Inclusions criteria were persistent increase of serum iron and serum transferrin saturation (>50%) at two separate tests, and LIC > 100 $\mu\text{mol/g}$. Exclusion criteria were HFE C282Y homozygous mutation, history of transfusion, bloodletting, hematological disease, or history of iron supplementation. Coding sequence of the genes *HAMP*, *HJV*, *TFR2*, *HFE*, *SLC40A1* and *BMP6* were sequenced. Serum hepcidin levels were determined with an enzyme immunoassay (Peninsula Laboratories, Bachem, San Carlos USA).

The third cohort was added to expand the recruitment of BMP6 patients. It included 10 consecutive patients (seven Caucasians, two African and one Asian) referred to the Gastroenterology department of Louis Mourier Hospital (Colombes, France) for unexplained hyperferritinemia and elevated LIC. We performed targeted next-generation sequencing (NGS) workflow based on a custom AmpliSeq panel sequencing most prevalent genes involved in iron disorders on the Ion PGM™ Sequencer.

DNA ANALYSIS

DNA was prepared from peripheral blood leukocytes using QIAamp DNA Blood Mini Kit (Qiagen). *BMP6* gene 7 exons and flanking sequences were amplified by PCR. The two strands of PCR products were sequenced with use of the BigDye Terminator Cycle Sequencing Ready Reaction kit on an ABI PRISM 3130xl sequencer (Applied Biosystems). *BMP6* sequencing primers (M13 tailed) are shown in supplementary Table S2.

HAPLOTYPE ANALYSIS

Haplotype analysis was performed with two microsatellite markers surrounding *BMP6* gene (22_AC and 16_GT, supplementary Table S2). Polymerase chain reactions (PCRs) were performed using 20 ng of genomic DNA and the products were analyzed using the ABI Prism 3130 Genetic Analyzer and Gene Mapper analysis software v4.0 (Life technologies).

BMP6 CONSTRUCTIONS AND MUTAGENESIS

BMP6 (NM_001718) Human cDNA previously inserted in pCMV6-Entry (ORF Myc-DDK tagged) was purchased from OriGene (catalogue N°: RC212307, BMP6-WT). All BMP6-Mutations were performed using site-directed mutagenesis (*Stratagene, La Jolla, CA, USA*). For functional studies, Myc-DDK sequences were removed by introducing the initial stop codon TAA at the C-terminal tail of BMP6-WT and mutants cDNAs. For dimerization test studies, the coding sequence of the human *BMP6* gene was amplified from a cloned full-length cDNA purchased from Open Biosystems (clone ID: clone ID: BC160106: 100064138). The PCR fragment was subcloned into the pcDNA3.1/V5-HIS-TOPO vector (V5-BMP6) according to the manufacturer's instructions (Life Technologies, Cergy Pontoise, France). Primers sequences are shown in supplementary Table S2.

IMMUNOHISTOCHEMICAL TESTING

Liver tissue samples were fixed in 10% formalin buffer, embedded in paraffin, sectioned, and stained with Perls' Prussian blue or with the primary anti-BMP6 (S-20) antibodies (1/50; Santa Cruz Biotechnology, inc. CliniSciences, Nanterre, France) diluted in PBS-1% BSA and 1% FCS. Immunohistochemistry was performed using an automated immunohistochemical stainer according to the manufacturer's guidelines (streptavidin-peroxidase protocol, BenchMark, Ventana).

CELL ANALYSES

Opossum Kidney (OK) cells (ATCC®, LGC STANDARDS, Molsheim, France) were cultured in Eagle's Minimum Essential Medium (EMEM) (ATCC®, LGC STANDARDS, Molsheim, France) containing 10% fetal calf serum (FCS), 100 U/ml penicillin, and 100 µg/ml streptomycin (Invitrogen-Gibco). HepG2 cells (ATCC®, LGC STANDARDS, Molsheim, France) were grown in

DMEM supplemented with 10% FBS, 100 U/mL penicillin, and 100 µg/mL streptomycin. HuH7 cells were cultured in DMEM with L-glutamine and 1 g/L glucose, supplemented with 10% heat decomplemented FBS, 100 U/mL penicillin, and 100 µg/mL streptomycin (Invitrogen-Gibco). The human hepatocarcinoma cell line Hep3B (ATCC®, LGC STANDARDS, Molsheim, France) was grown in DMEM, 10% fetal calf serum, 100 U/mL penicillin, and 100 µg/mL streptomycin (Invitrogen-Gibco). All cell lines were transfected using the X-tremGENE HP DNA Transfection Reagent (Roche Diagnostics, Mannheim, Germany), according to manufacturer's instructions. Transfected culture were then washed and maintained in the serum-free medium until reaching confluence (1-2 days after transfection).

Transfected OK cells were used to produce secreted forms of WT and mutated BMP6 proteins. The resulting conditioned medium was used to treat HepG2, Hep3B and HuH7 cells for an additional 24 hours. Cells were then harvested and the cellular extract was used to quantify mRNAs or proteins levels. For SMAD signaling, HepG2 cells underwent early incubation (5 min to 90 min) with the conditioned medium and then they were immediately processed to evaluate the phosphorylation level of Smad1/5/8 by immunoblotting.

CONFOCAL MICROSCOPY

Transfected and confluent OK were washed 3 times with PBS, fixed for 10 minutes at room temperature with 3% paraformaldehyde, washed again 3 times with PBS, incubated with 20 mmol/L glycine for 10 minutes, and subsequently permeabilized for 30 min with PBS containing 0.1% saponin. The actin staining was performed with Alexa Fluor 635 phalloidin (1/200, for 30 minutes at room temperature). The BMP6-WT and mutated proteins staining was performed with anti-BMP6 or anti-DDK antibodies (OriGene, by CliniSciences, France, Nanterre). The coverslips were mounted by using DAKO-glycerol containing 2.5% 1,4-diazabicyclo- (2.2.2) octane (Sigma Aldrich, St Louis, MO) as a fading retardant. Confocal images were taken with a high-resolution confocal biophoton microscopy Leica SP8 (Saint Jorioz, France) equipped with 60x oil-immersion objectives.

IMMUNOBLOTTING AND IMMUNOPRECIPITATION

For protein cell extraction, cells were harvested by incubation during 60 min in ice-cold RIPA buffer (0.05 M Tris-HCl at pH 7.6, 0.15 M NaCl, 1% w/v Triton X-100, 0.1% SDS, 1mM EDTA) containing 1x protease inhibitor cocktail (Complete, Roche). The cell lysates were then centrifuged at 4°C x 12,000 g for 15 min to recover the protein pellet. For secreted proteins, the serum free-supernatants were filtered through centrifugal filter unit (Amicon Ultra-4 centrifugal filters, Millipore, Paris, France) and concentrate samples were recovered and stored. Protein concentrations were measured by Bradford assay (Bio-Rad). For the immunoblot, the proteins (10 to 60 µg) were

separated by electrophoresis on 10-12% SDS-polyacrylamide mini-gel and subsequently electrotransferred to nitrocellulose membranes (Mini Trans Blot Module, Bio-Rad). Loading and transfer efficiency were systematically checked by Ponceau red staining (ponceau S) of the membranes. The membranes were incubated overnight with primary antibodies (1:500 dilution for rabbit anti phospho-Smad1/5/8 (Millipore Paris, France) and 1:1000 dilutions for goat anti-BMP6. Immunoreactive bands were revealed by HRP-conjugated Secondary antibodies and with Amersham ECL. The quantification was represented as ratio of BMP6 protein level on the level of the 72 kDa band revealed by Ponceau R. We used this band that was systematically revealed in all our blots.

For immunoprecipitation (IP) studies, OK cells were cotransfected with equal amounts of constructs expressing V5-tagged WT BMP6 (pcDNA3.1-V5, life technologie, invitrogen sarl, France, Cergy Pontoise) alone or along with WT BMP6 or Leu96Pro-BMP6. 2 days after transfection, both cell pellet and conditioned supernatant were incubated in lysis buffer. One mL aliquots of lysates (500 µg of proteins) were immunoprecipitated by incubation with 2 µg of anti-DDK antibody, anti-V5 antibody or an isotype IgG and 100 µL of protein A-agarose overnight at 4 °C on a rocking platform. Proteins were processed for 10-12 % SDS-polyacrylamide page and the immunoblot. The membranes were incubated overnight with HRP-conjugated primary anti-V5-HRP antibody (1/5000, Life Technologie, invitrogen sarl, France, Cergy Pontoise) or with anti-DDK antibody and immunolabeling was detected directly using the ECL reagent (Amersham Biosciences).

RNA EXTRACTION AND QUANTITATIVE REAL-TIME PCR

Total RNA was isolated from cultured cells using RNA-PLUS™ reagent (MP-Europe) according to the manufacturer's recommendations. Complementary DNA was synthesized using oligo(dT) primer and Moloney Murine Leukaemia Virus reverse transcriptase (invitrogen sarl, France, Cergy Pontoise) as per the manufacturer's instructions, using 2 µg total RNA template per sample. Reverse transcriptase quantitative polymerase chain reaction (RT-qPCR) was performed with specific sets of primers and LightCycler 480 DNA SYBR Green I Master Mix applying (Roche Diagnostics, Mannheim, Germany) and run on a LightCycler 780 Instrument (Roche Diagnostics). *HAMP* and *Id1* and *BMP6* transcripts were amplified with specific primers (supplementary Table S1). In parallel, β 2M transcripts were amplified with specific primers and detected in a similar manner to serve as an internal control. Standard curves for *HAMP*, *Id1*, *BMP6* and β 2M were generated from accurately determined dilutions of cDNA. Samples were analysed in duplicate for each experiment, and results are reported as the ratio of mean values for hepcidin or *Id1* to β 2M.

STATISTICAL ANALYSIS

A two-tailed Student's t-test and Chi-square test were used with a P value of < 0.05 determining statistical significance. 95% confidence intervals for the odds ratio were calculated. GraphPad InStat software (GraphPad Software, San Diego, CA) was used for statistical evaluation.

RESULTS

Patient characteristics

In a cohort of 70 patients with moderate unexplained iron overload, we found six individuals, five males and one female, carrying one heterozygous *BMP6* mutation. The most relevant clinical and biological data of these patients are shown in Table 1. The patients were over 50 years of age (mean age 57.5, 50-65), with elevated serum ferritin, normal or high transferrin saturation and elevated LIC. Perl's staining of the liver biopsies from patient 4 showed significant iron overload in both hepatocytes and Kupffer cells (Figure 1D). Five out of six patients were treated through phlebotomy, removing 1.5-5 g of total iron. Serum hepcidin was measured through LC-MSMS spectrometry. Although the results were not available for all patients, the patients with *BMP6* mutations had normal or only slightly elevated serum hepcidin levels, despite the presence of excess liver iron (Table 1). Family studies were performed for five patients (Figure 2) and additional carriers of a mutation were identified, some of them also showing moderate signs of iron overload (Patient II.2, Family 5). We also measured serum hepcidin in two young asymptomatic carriers available (III.1 and 2, family 1) who exhibited normal iron status. Their serum hepcidin levels were normal (data not shown).

Altogether, these results suggested that these heterozygous *BMP6* mutations conferred susceptibility to iron overload, although younger carriers were not iron overloaded and women appeared to be protected from iron overload. They also appeared to aggravate the iron load resulting from additional factors such as overweight (proband 4, LIC 230 $\mu\text{mol/g}$) or moderate alcohol intake (proband 5, LIC 220 $\mu\text{mol/g}$), two conditions known to lead to moderate iron excess (LIC<150 $\mu\text{mol/g}$ [24]).

Identification of *BMP6* mutations

The *BMP6* mutations that we identified were located in exon 1: c.283C>T (p.Pro95Ser, one patient), c.287T>C (p.Leu96Pro, three patients), and c.337C>G (p.Gln113Glu, two patients). These three mutations were located in the propeptide domain and affected amino acids highly conserved throughout species (Figure 1 A-C). These three *BMP6* mutations were also present in some individuals of European American Caucasian descent (39 out of \approx 8000 alleles) found in the Exome Variant Server (<http://evs.gs.washington.edu/EVS/>, see supplementary Table S3), albeit at a nine times lower frequency than in our cohort of patients (6 out of 140 alleles, $P<0.00001$). Thus, *BMP6* mutations were highly associated with an iron overload phenotype in the studied patients (OR 9.62,

95 % CI 3.93, 23.52, $P < 0.0001$). In a conservative hypothesis, when all mutations found in the propeptide in EVS controls are taken into account (51 out of ≈ 8000 alleles, supplementary Table S3) the difference of frequency between patients and EVS controls remains highly significant ($P < 0.00001$, OR 6.84, 95 % CI 2.84, 15.92,). We also sequenced *BMP6* propeptide in 200 healthy French Caucasian controls and found solely one heterozygous synonymous coding mutation in one subject. The difference of frequency between patients and our 200 controls was also significant ($P < 0.05$, OR 40.41, 95%CI 2.25, 727.23,).

For the three patients with the p.Leu96Pro, based on the study of polymorphic SNPs in the *BMP6* gene region we could not exclude a founder effect for p.Leu96Pro mutation. We therefore, performed haplotype analysis in families 2, 3, and 4 with two microsatellites markers surrounding *BMP6* gene (see supplementary figure S1). We found that eight patients who carried the *BMP6* p.Leu96Pro mutation did not share a unique haplotype, consistent with the hypothesis of multiple independent mutational events.

Replication cohort analysis

Sixty two patients were initially included. Two of them were later excluded, one because of HFE p.Cys282Tyr homozygous mutation found at sequencing and one because of low serum transferrin saturation at inclusion. One patient (R1) had the p.Leu96Pro mutation (table 1). She presented metabolic syndrome with diabetes, porphyria cutanea tarda and the HFE p.His63Asp mutation. As in proband 4 and proband 5 of the first cohort, the presence of the *BMP6* mutation seemed to exacerbate the liver iron overload (250 $\mu\text{mol/g}$), over the level normally observed in metabolic syndrome [24]. Although one cannot rule out the possibility that p.His63Asp HFE mutation might contribute to the accumulation of excess iron in the liver, this mutation is not usually considered as pathogenic in the absence of the p.Cys282Tyr mutation [25]. One patient (R2) had the p.Gln113Glu mutation (table 1). He had no other comorbidities than moderate dyslipidemia and presented with elevated serum ferritin and serum transferrin saturation since three years.

Additional cohort analysis

Ten patients were initially included. We identified one Caucasian patient with only one heterozygous p.Leu96Pro *BMP6* mutation without any modification in the other genes. We confirmed the presence of this mutation by Sanger sequencing and verified that *HFE*, *HJV*, *TFR2*, *HAMP* and *SLC40A10* genes were not affected. The patient exhibited signs of moderated iron overload including elevated serum ferritin (968 $\mu\text{g/L}$), transferrin saturation (52%) and LIC (95 $\mu\text{mol/g}$). Family history of this patient showed that his son also exhibited an unexplained hyperferritinemia.

Functional analysis of *BMP6* mutations

Because the mutations identified in the patients studied were all located in the propeptide region, we expected these mutations to alter BMP6 protein folding and/or secretion. When we analyzed the BMP6 staining in the liver biopsies obtained from patient 4, we observed reduced levels of BMP6 protein in hepatocytes compared with control biopsies (Figure 3A), with apparent protein retention in the compartments surrounding the nucleus. We tried to measure the protein level of BMP6 in the serum of patients, but we found that circulating BMP6 was undetectable both in BMP6 patients and in healthy individuals confirming the accepted assumption of a local synthesis and an autocrin/paracrin effect of BMP6. Thus, we performed additional *in-vitro* studies to obtain further insight into the functional consequences of the BMP6 mutations. For the immunolocalization studies, we transfected OK cells with plasmids expressing the DDK-BMP6 fusion proteins and stained the transfected cells with either the BMP6 antibody (see supplementary figure S2), or an antibody against the DDK peptide (Figure 3B) to avoid detecting the endogenous BMP6 protein. BMP6-WT showed uniform labeling whereas the BMP6-mutants were primarily accumulated in cytosolic aggregates similar to that observed in the liver of patient 4, confirming the impairment of BMP6 secretion.

Protein expression analysis of WT and mutated BMP6 was additionally performed by immunoblotting. OK cells were transfected with WT and mutant BMP6-expressing vectors. Equal mRNA levels of transfected BMP6-WT and mutants were observed, confirming equal transfection efficiency of the various constructs (Figure 4A). The level of the mature form of BMP6-mutants (Figure 4B) was significantly decreased compared with the WT in both cell extracts (C) and the secreted fractions (S). However, in contrast to BMP6-WT, the high molecular weight (HMW) form of BMP6-mutants was slightly accumulated in the (C) fractions (Figure 4 B-C), although total amount of BMP6 remained significantly reduced (Figure 4C). These data suggest that BMP6-mutants are likely to be retained in quality control compartments and subsequently degraded.

Because BMP6 induces phosphorylation of SMAD1/5/8 proteins, we examined whether this pathway was affected through BMP6 mutations. When HepG2 cells were incubated with conditioned media derived from OK cells previously transfected with BMP6-expressing plasmids, we observed the induction of a rapid phosphorylation by BMP6-WT treatment, with a maximum after 1 hour (Figure 5A). However, the kinetics of SMAD1/5/8 activation was not altered with the p.Leu96Pro mutant, although the extent of the phosphorylation was reduced compared with BMP6-WT. Furthermore, conditioned medium from cells transfected with the p.Leu96Pro-mutant induced

only a 10-fold increase in *HAMP* mRNA, differing significantly from the 50-fold increase induced with the WT protein (Figure 5B). The expression of the *Id1* gene, another BMP6 target, in the same samples was identical to that of *HAMP*, confirming the reduced functional activity of the BMP6 mutants (Figure 5B). Similar data were obtained for p.Pro95Ser and p.Gln113Glu BMP6 mutants (Supplementary Figure S3). These data were additionally confirmed in two other hepatocyte cell lines Hep3B (Figure 5C) and HuH7 (Supplementary Figure S3).

Furthermore, because BMP6 assembles as a dimer and patients carrying mutations are heterozygotes, we co-expressed BMP6-WT and the p.Leu96Pro-mutant in HepG2 cells. The mutated protein co-expressed with BMP6-WT failed to induce hepcidin production to the same extent as the mutated protein alone compared with BMP6-WT alone (Figure 6A), suggesting a dominant-negative mechanism. Therefore, we investigated whether BMP6 mutants interact with BMP6-WT. We co-transfected OK cells with constructs expressing V5-BMP6 along with BMP6-WT (DDK-WT) or with pLeu96Pro-BMP6 (DDK-M). Immunoprecipitation (IP) and Western blotting were then performed as described in methods. Figure 6B clearly showed that similarly to BMP6-WT, pull-down of DDK-M using anti-DDK antibody results in co-precipitation of V5-BMP6. Co-IP controls confirming specificity of the interaction between WT and mutated-BMP6 proteins (including isotype IgG control and cells in which only V5-BMP6 was transfected and then anti-DDK immunoprecipitation was performed) are shown in Supplementary Figure S4. These results suggest that despite the mutation, BMP6 mutants conserved their ability to form heterodimers with BMP6-WT. Thus, we hypothesized that BMP6 mutations may lead to intracellular retention of WT/mutant heterodimer proteins. Taken together, these data suggested that BMP6 propeptide mutations might reduce BMP6 secretion, thereby leading to impaired hepcidin production in the liver.

DISCUSSION

In the present study, we report for the first time that heterozygous *BMP6* defects in humans can lead to a mild to moderate late-onset iron overload phenotype, showing both elevated serum ferritin levels and increased liver iron stores. These observations differed from those in mice, where homozygous *Bmp6* inactivation induced severe iron overload [20,22]. However, in the present study, the patients were heterozygous for the *BMP6* defect, and the mutation induced a change in the propeptide region that did not fully inactivate the protein. This new *BMP6*-related disorder resembled classical hemochromatosis in several respects: there were more affected males than females, iron excess was present only in carriers of *BMP6* mutations aged 50 years and over, and the extra iron load was efficiently removed by therapeutic phlebotomies. However, this disorder also differed from classical hemochromatosis in that transferrin saturation was not consistently increased, and the patients did not exhibit clinical symptoms of iron overload and were

heterozygotes for the causing mutations. We propose that a dominant-negative effect of the mutated allele on the processing of the BMP6-WT (as suggested by data in Figure 6) might be sufficient to favor iron overload. Indeed, the mature BMP6 protein requires the formation of heterologomeric complexes with the cleaved propeptide for optimal secretion and trafficking within the cell [19,26,27]. The results of the *in vitro* studies showed that BMP6 proteins mutated in the propeptide exhibited impaired secretion with intracellular retention leading to the diminished activation of downstream effectors. These data are consistent with reports showing that most of *TGF- β I* gene mutations responsible for autosomal-dominant Camurati-Engelmann disease (MIM 131300) are located in the propeptide domain, leading to the intracellular retention and impaired secretion of the mutated protein[28]. Notably, the appropriate secretion and activation of BMPs also requires the formation of homodimers or heterodimers with other BMPs [19,29,30]. Thus, it is possible that other mechanisms, such as impaired dimer formation with BMPs or diminished BMP activation contribute to the reduced activity of BMP6 mutants.

Two other lines of evidence support the implication of these BMP6-propeptide mutations in defective iron signaling and lack of hepcidin response. First, our *in vitro* experiments showed that the amount of BMP6 secreted in the culture medium of cells transfected with mutated BMP6 was not sufficient to fully activate the SMAD1/5/8 signaling pathway and therefore only partially induced hepcidin synthesis (Figure 5 and Supplementary Figure S4). Second, we also observed normal or slightly elevated serum hepcidin levels in *BMP6* patients, which were inappropriately low considering the patient iron load. These results are similar to those of previous studies showing the presence of normal or only slightly elevated serum hepcidin levels in *HFE*-HH patients, despite the presence of excess liver iron[31-33]. Interestingly, the level of SMAD phosphorylation has also been reported to be inappropriately low in *HFE* hepatocytes[34]. Together with previously published data, these results highlight the importance of the BMP pathway in iron signaling and hepcidin response in humans. Indeed, a significant association has already been detected between serum ferritin level and a common single-nucleotide polymorphism in the *BMP2* genic region in *HFE* patients[35] and a mutation in the BMP-response element of the *HAMP* promoter has been observed in patients with HH[36].

In conclusion, the results of the present study show that these propeptide BMP6 mutations are responsible for inappropriate hepcidin response and mild to moderate iron overload in some patients with so-called unexplained hyperferritinemia. We propose that *BMP6* is a new susceptibility gene for iron overload in Caucasians and speculate that it could be the principal susceptibility gene in other ethnic groups where *HFE* mutations are rarely present²⁵. Indeed, several rare *BMP6* missense variants present in African American control populations from the Exome Variant Server are likely deleterious. Nevertheless, additional studies with larger cohorts are required to assess the exact

frequency of *BMP6*-related iron overload. In addition, the presence of *BMP6* variants in the general population, albeit at a low frequency, opens up the possibility that *BMP6* could also act as a modifier gene of HFE-related hemochromatosis where the degree of iron overload is highly variable[4,5,13] or could aggravate the accumulation of excess iron in common diseases such as metabolic syndrome or alcoholism.

ACCEPTED MANUSCRIPT

REFERENCES

1. Brasse-Lagnel C, Karim Z, Letteron P, et al. Intestinal DMT1 cotransporter is down-regulated by hepcidin via proteasome internalization and degradation. *Gastroenterology* 2011;140:1261-1271 e1.
2. Delaby C, Pilard N, Goncalves AS, et al.. Presence of the iron exporter ferroportin at the plasma membrane of macrophages is enhanced by iron loading and down-regulated by hepcidin. *Blood* 2005;106:3979-84.
3. Ganz T, Nemeth E. Hepcidin and iron homeostasis. *Biochim Biophys Acta* 2012;1823:1434-43.
4. Brissot P, Bardou-Jacquet E, Jouanolle AM, et al.. Iron disorders of genetic origin: a changing world. *Trends Mol Med* 2011;17:707-13.
5. Fleming RE, Ponka P. Iron overload in human disease. *N Engl J Med* 2012;366:348-59.
6. Adams PC, Barton JC. Haemochromatosis. *Lancet* 2007;370:1855-60.
7. D'Alessio F, Hentze MW, Muckenthaler MU. The hemochromatosis proteins HFE, TfR2, and HJV form a membrane-associated protein complex for hepcidin regulation. *J Hepatol* 2012;57:1052-60.
8. Nicolas G, Chauvet C, Viatte L, et al.. The gene encoding the iron regulatory peptide hepcidin is regulated by anemia, hypoxia, and inflammation. *J Clin Invest* 2002;110:1037-44.
9. Nemeth E, Rivera S, Gabayan V, et al.. IL-6 mediates hypoferrremia of inflammation by inducing the synthesis of the iron regulatory hormone hepcidin. *J Clin Invest* 2004;113:1271-6.
10. Guillem F, Lawson S, Kannengiesser C, et al.. Two nonsense mutations in the TMPRSS6 gene in a patient with microcytic anemia and iron deficiency. *Blood* 2008;112:2089-91.
11. Silvestri L, Guillem F, Pagani A, et al.. Molecular mechanisms of the defective hepcidin inhibition in TMPRSS6 mutations associated with iron-refractory iron deficiency anemia. *Blood* 2009;113:5605-8.
12. **De Falco L, Sanchez M**, Silvestri L, et al.. Iron refractory iron deficiency anemia. *Haematologica* 2013;98:845-53.
13. Pietrangelo A. Hereditary hemochromatosis--a new look at an old disease. *N Engl J Med* 2004;350:2383-97.
14. Pietrangelo A, Caleffi A, Corradini E. Non-HFE hepatic iron overload. *Semin Liver Dis* 2011;31:302-18.
15. Pietrangelo A. Non-HFE hemochromatosis. *Semin Liver Dis* 2005;25:450-60.
16. Montosi G, Donovan A, Totaro A, et al.. Autosomal-dominant hemochromatosis is associated with a mutation in the ferroportin (SLC11A3) gene. *J Clin Invest* 2001;108:619-23.
17. Njajou OT, Vaessen N, Jousse M, et al.. A mutation in SLC11A3 is associated with autosomal dominant hemochromatosis. *Nat Genet* 2001;28:213-4.
18. Hetet G, Devaux I, Soufir N, et al.. Molecular analyses of patients with hyperferritinemia and normal serum iron values reveal both L ferritin IRE and 3 new ferroportin (slc11A3) mutations. *Blood* 2003;102:1904-10.
19. Bragdon B, Moseychuk O, Saldanha S, et al.. Bone morphogenetic proteins: a critical review. *Cell Signal* 2010;23:609-20.
20. **Andriopoulos B, Jr., Corradini E, Xia Y**, Faasse SA, et al.. BMP6 is a key endogenous regulator of hepcidin expression and iron metabolism. *Nat Genet* 2009;41:482-7.
21. Babitt JL, Huang FW, Wrighting DM, et al.. Bone morphogenetic protein signaling by hemojuvelin regulates hepcidin expression. *Nat Genet* 2006;38:531-9.
22. **Meynard D, Kautz L**, Darnaud V, et al.. Lack of the bone morphogenetic protein BMP6 induces massive iron overload. *Nat Genet* 2009;41:478-81.

23. Lefebvre T, Dessendier N, Houamel D, et al. development of a LCMS/MS method for hepcidin-25 measurement in Human and mouse serum: clinical and research implications in iron disorders. *clin chem lab med* 2015; DOI 10.1515/cclm-2014-1093.
24. Deugnier Y, Brissot P, Loreal O. Iron and the liver: update 2008. *J Hepatol* 2008;48 Suppl 1:S113-23.
25. Adams PC, Reboussin DM, Barton JC, et al.. Hemochromatosis and iron-overload screening in a racially diverse population. *N Engl J Med* 2005;352:1769-78.
26. Gray AM, Mason AJ. Requirement for activin A and transforming growth factor--beta 1 pro-regions in homodimer assembly. *Science* 1990;247:1328-30.
27. Shi M, Zhu J, Wang R, Chen X, et al.. Latent TGF-beta structure and activation. *Nature* 2011;474:343-9.
28. Janssens K, Vanhoenacker F, Bonduelle M, et al.. Camurati-Engelmann disease: review of the clinical, radiological, and molecular data of 24 families and implications for diagnosis and treatment. *J Med Genet* 2006;43:1-11.
29. Israel DI, Nove J, Kerns KM, et al.. Heterodimeric bone morphogenetic proteins show enhanced activity in vitro and in vivo. *Growth Factors* 1996;13:291-300.
30. Little SC, Mullins MC. Bone morphogenetic protein heterodimers assemble heteromeric type I receptor complexes to pattern the dorsoventral axis. *Nat Cell Biol* 2009;11:637-43.
31. Ganz T, Olbina G, Girelli D, et al.. Immunoassay for human serum hepcidin. *Blood* 2008;112:4292-7.
32. Girelli D, Trombini P, Busti F, et al.. A time course of hepcidin response to iron challenge in patients with HFE and TFR2 hemochromatosis. *Haematologica* 2010;96:500-6.
33. Ravasi G, Pelucchi S, Trombini P, et al.. Hepcidin expression in iron overload diseases is variably modulated by circulating factors. *PLoS One* 2012;7:e36425.
34. Ryan JD, Ryan E, Fabre A, et al.. Defective bone morphogenic protein signaling underlies hepcidin deficiency in HFE hereditary hemochromatosis. *Hepatology* 2010;52:1266-73.
35. **Milet J, Dehais V**, Bourgain C, et al.. Common variants in the BMP2, BMP4, and HJV genes of the hepcidin regulation pathway modulate HFE hemochromatosis penetrance. *Am J Hum Genet* 2007;81:799-807.
36. Island ML, Jouanolle AM, Mosser A, et al.. A new mutation in the hepcidin promoter impairs its BMP response and contributes to a severe phenotype in HFE related hemochromatosis. *Haematologica* 2009;94:720-4.

Author names in bold designate shared co-first authorship

FIGURE LEGENDS

Figure 1. BMP6 Mutations and iron overload in a liver biopsy of a patient with the p.Leu96Pro mutation. A: schematic representation of the BMP6 protein. The three mutated residues identified in patients are located in the propeptide domain. B: sequence alignment of amino-acids 90 to 138 showing that the mutated residues (in red) are highly conserved between species. C: chromatogram of the nucleotide sequence within exon 1 of *BMP6* gene with nucleotides indicated above the curves. D: Perl's staining of the liver biopsy sections of patient 4 (p.Leu96Pro mutation). Significant iron overload was observed in both hepatocytes (H) and Kupffer cells (K). the scale bars: 30 μ m.

Figure 2. Family studies and pedigrees of each of the five probands with *BMP6* mutation.

Pedigrees were drawn for each proband. Squares indicate male family members, circles female family members, black symbols probands and carriers with biological signs of iron overload, white symbols with black line asymptomatic mutation carriers and white symbols non carriers; slashes indicate deceased family members. Arrows indicate the proband. Biological data of family members are shown in rectangular boxes, when available. A: age, I: serum iron (10-30 μ M), F: serum ferritin (F 5-105, M 30-300 μ g/L), TS; transferrin saturation (20-45%), LIC: MRI hepatic iron (N<36 μ mol/g). ND not determined.

Figure 3. Intracellular location of missfolded BMP6 mutants:

A: BMP6 protein expression in the liver biopsies of patient 4 (lower panel) and a healthy control (upper panel). Arrows indicate apparent cytosolic aggregates of mutated BMP6 protein. B: subcellular location of BMP6-WT and mutants in OK cells transfected with the corresponding plasmid expressing the DDK-tagged fusion protein. These cells were subsequently fixed and DDK-BMP6 proteins were immunostained with anti-DDK antibody (green). The actin and nucleus were stained with Alexa Fluor 635 phalloidin (red) and Hoechst dye (blue) respectively. The images show the abnormal accumulation of the p.Leu96Pro mutant protein in intracellular compartments. The scale bars: 100 μ m and 30 μ m for biopsies and confocal images respectively.

Figure 4. mRNA and protein level of expressed BMP6-WT and mutants.

OK cells were transfected with BMP6 constructs and then the cell extracts (C) and/or supernatants (S) were prepared to assess the expression of BMP6-mRNA and/or protein respectively. A: showed the mRNA level of BMP6-WT (WT) and mutants (p.Pro95Ser, p.Leu96Pro, p.Gln113Glu). The data were normalized to 1 μ g of total RNA and reported as the mean \pm sem (n=3 in each experience). B: Representative images of the abundance of BMP6-WT (1), p.Pro95Ser (2), p.Gln113Glu (3), and p.Leu96Pro (4) proteins detected through immunoblotting. The amount of the

protein loading was systematically visualized through Ponceau red staining (Ponceau S). C: Summarizes the quantifications of the ratio of BMP6 signals on a 72 kDa protein of Ponceau S. The amount of mature BMP6-mutants (expected molecular weight 18-23 kDa according to the extent of N-linked glycosylation) is reduced both in (C) and (S), as compared to BMP6-WT. However, the amount of the high molecular weight propeptide (HMW, Predicted at 57 kDa) is increased in (C). The data are mean \pm sem (n=4 experiences). *P < 0.05, **P < 0.01, ***P < 0.001.

Figure 5. Functional studies of BMP6 mutations in-vitro.

A: Induction of SMAD1/5/8 signaling. OK cells were transfected with plasmids expressing BMP6-WT (WT) or the p.Leu96Pro-mutant (M). The supernatants were used as conditioned medium to treat confluent HepG2 cells. The kinetics was established for 5-90 min, and the level of SMAD phosphorylation was evaluated through immunoblotting using anti-pSmad1/5/8 antibody (pSMAD). The amount of the protein loading was controlled through actin staining. Left panel shows representative immunot blot and right panel shows the quantification. B and C: Induction of *HAMP* and *Id1* mRNA-expression. OK cells were transfected with BMP6-WT or mutants. The conditioned medium was used to treat confluent HepG2 cells (B) or Hep3B (C) for 24 h. The mRNA levels were determined through RT-qPCR. The data were normalized to the levels of β 2-microglobulin (β 2M) mRNA and reported as the mean \pm sem (n=3 in each experience). *P < 0.05, **P < 0.01, ***P < 0.001, ns: not significant.

Figure 6. Protein dimerization between BMP6-WT and mutants.

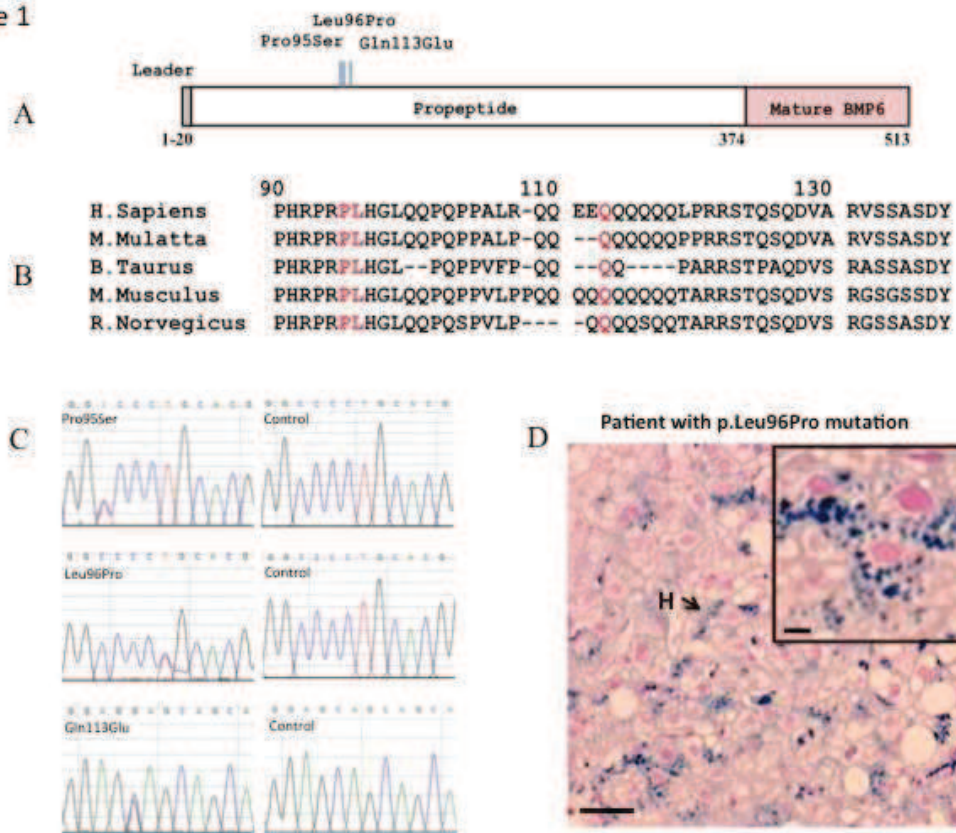
A: the effect of BMP6-WT (WT) or pLeu96Pro-mutant (M) alone on *HAMP* mRNA induction was compared to the effect of a combination of half the amount of each vector (WT+M, mimicking heterozygosity). Samples were analyzed in duplicate and reported as ratio of mean values for *HAMP*. Results are reported as the mean \pm sem (n=3 in each experiment). B: heterodimerization of BMP6-WT and M was explored by co-immunoprecipitation followed by Western blot analysis as described in methods. OK cells were transfected with the indicated plasmids and cell extracts (C) and conditioned medium (S) were immunoprecipitated with anti-DDK (IP:DDK). The Western blots were revealed by anti-V5-BMP6. Input blot (Input: DDK, 10% input) was also performed to ensure expression of DDK-proteins and V5-proteins in samples used for IP. The results showed association between BMP6-WT and pLeu96Pro-mutant monomers suggesting dominant-negative effect of BMP6 mutations.

Table 1: Clinical and biological data of the patients with BMP6 mutations

BMP6 Mutation	Initial cohort					Replication cohort		
	p.Pro95Ser (1 proband)	p.Leu96Pro (3 probands)			p.Gln113Glu (2 probands)		p.Leu96Pro (R1)	p.Gln113Glu (R2)
Gender	M	M	F	M	M	M	F	M
Weight (kg)/Height (m)	73/1.73	68/1.73	55/1.64	106/1.73	89/1.71	71/1.78	83/1.5	78/1.71
Age at diagnosis (y)	56	58	56	46	53	52	77	60
Transferrin saturation (%)	26	38	40	99	92	41	70	51
LIC*($\mu\text{mol/g}$)	170	55	70	230	220	200	250	160
Serum ferritin ($\mu\text{g/L}$) before/after phlebotomies	900/55	700/150	481/148	4000/680	2358/808	800/117	1430/nd	830/nd
Serum hepcidin by LCMSMS ($\mu\text{g/L}$) before/after phlebotomies	nd/16.4	32.9/nd	nd/7.6	30.6/nd	31.9/16.9	25/nd		
Serum hepcidin by ELISA ($\mu\text{g/L}$) before/after phlebotomies							38/nd	62/nd
Phlebotomies (mL)/iron removed (g)	nd	10x300 /1.5	10x250/1.2 5	20x500/5	8x500/2	14x500 /3.5	nd	nd
Clinical symptoms, other factors	Arthralgia	none	none	none	Alcohol	Arthralgia	Diabetes, porphyria cutanea tarda	dyslipidemia

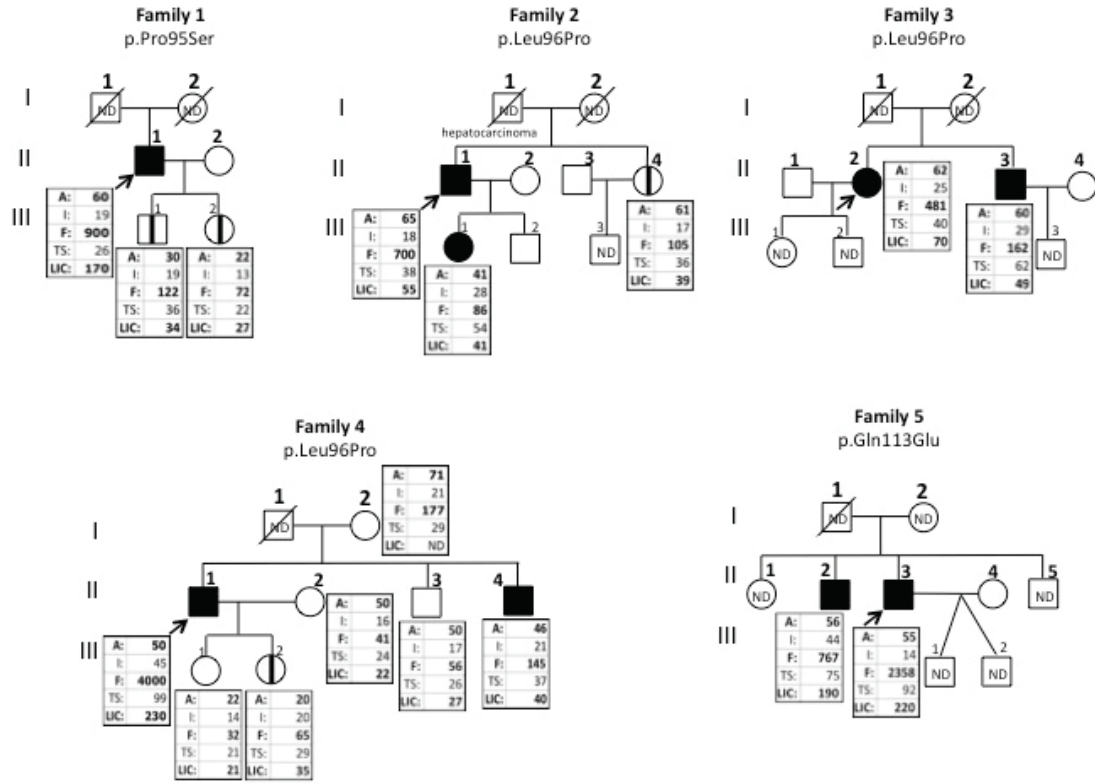
* Liver iron concentration (LIC) was determined by MRI; normal value < 36 $\mu\text{mol/g}$. Normal values: serum ferritin F 5-105, M 30-300 $\mu\text{g/L}$, % Tf saturation 20-45, serum hepcidin measured by LCMSM N < 19 $\mu\text{g/L}$, serum hepcidin measured by ELISA N: 4 – 30 $\mu\text{g/L}$.

Figure 1



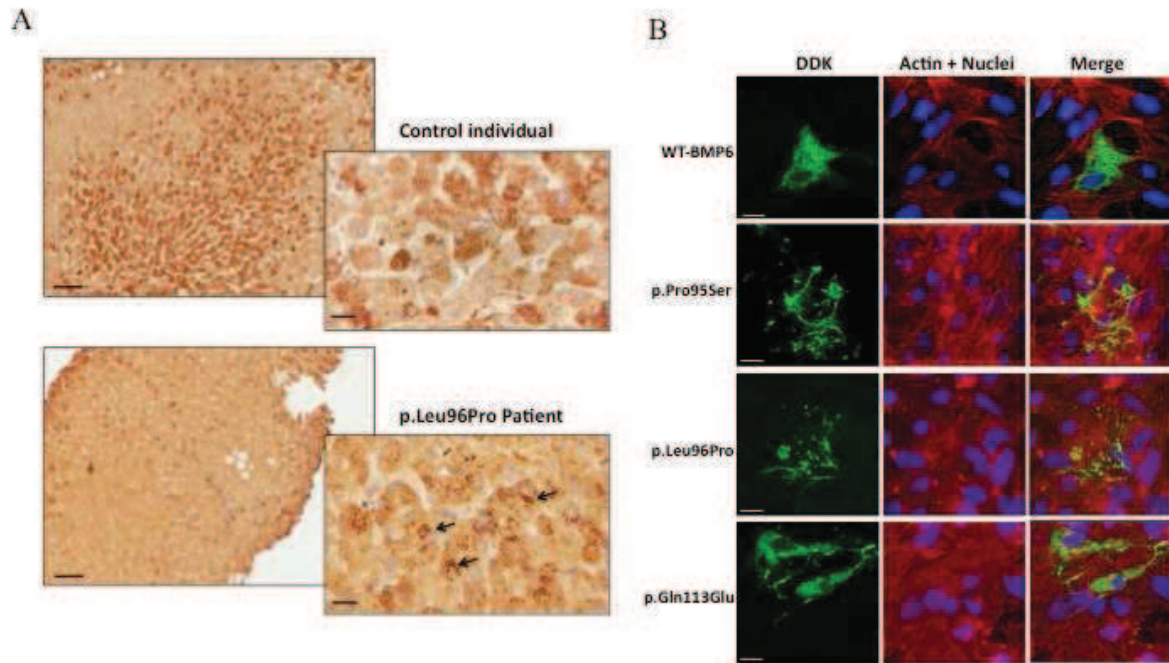
ACCEPTED TEL

Figure 2



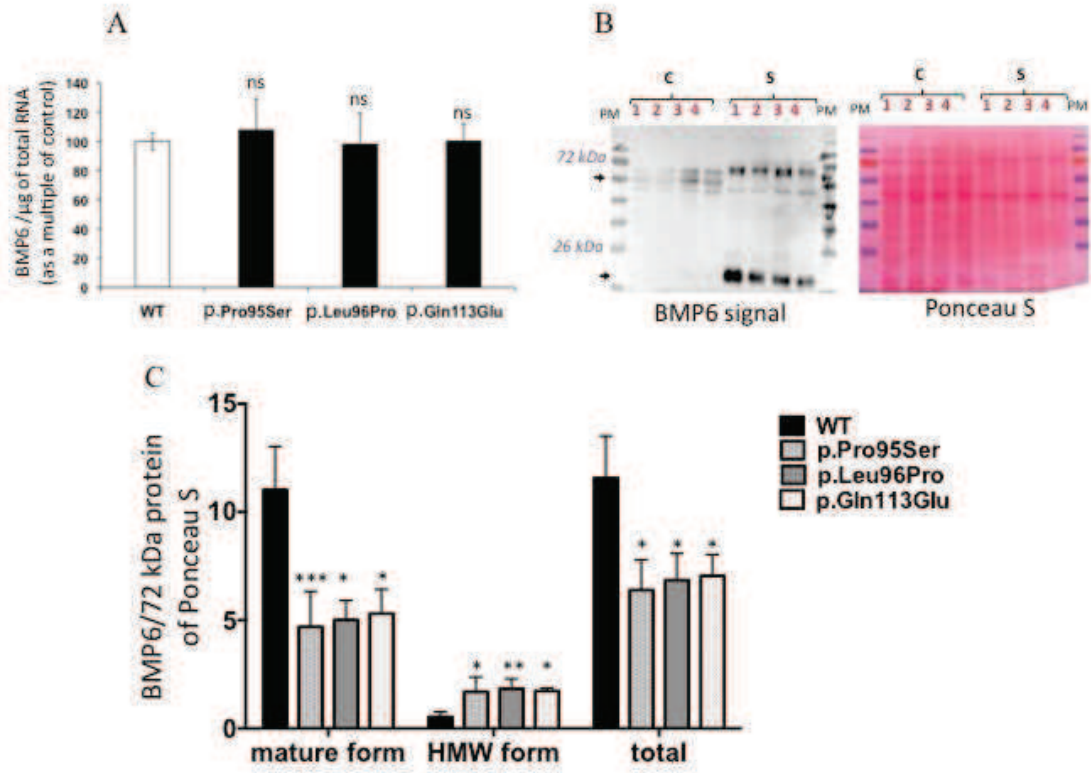
ACCEPTED TEL

Figure 3



ACCEPTED

Figure 4



ACCEPTED TEL

Figure 5

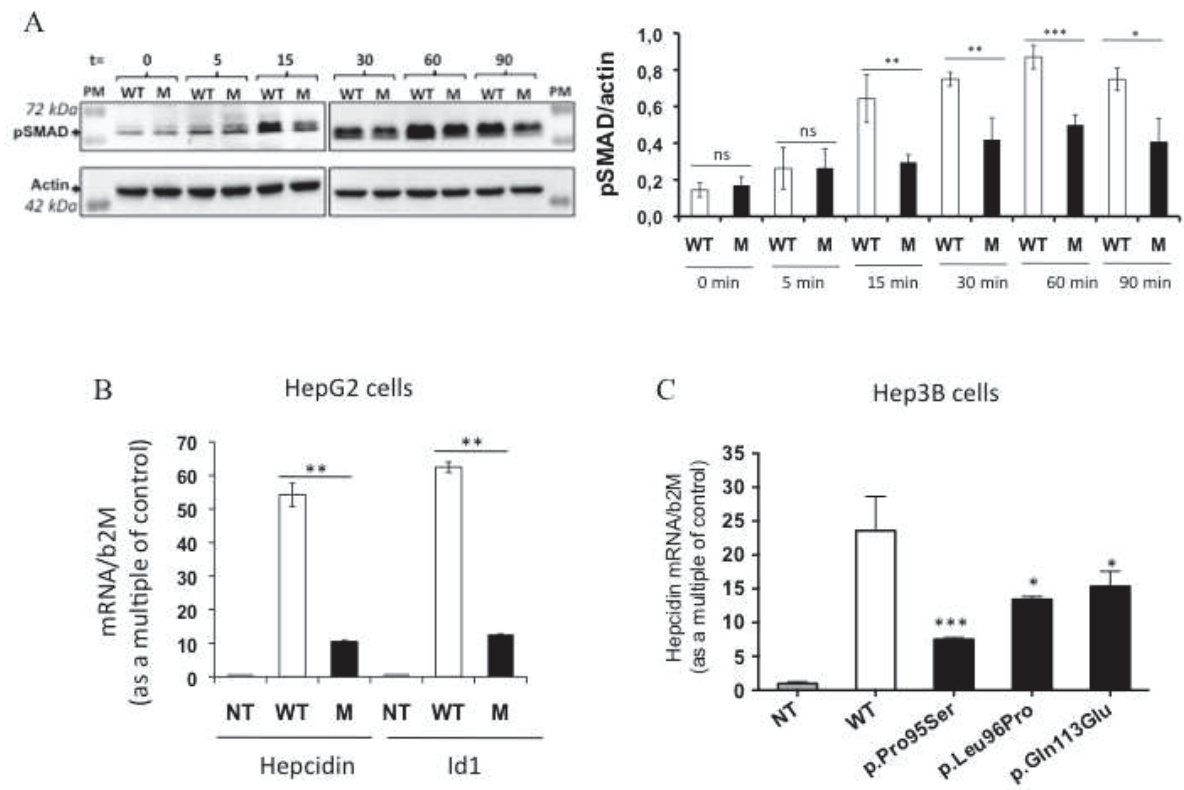


Figure 6

